

Calculation of Photo-Ionisation Cross Sections and Radiative Recombination Rate Coefficients for CO and CO⁺ Molecules

Raja DHOUIOUI^{1,2}, Philippe TEULET¹, Yann CRESSAULT¹, Hassen GHALILA², Riadh RIAHI², Nejm Eddine JAIDANE² and Zohra BEN LAKHDAR²

¹Université de Toulouse, UPS, INPT, LAPLACE (Laboratoire Plasma et Conversion d'Énergie), 118 route de Narbonne, F-31062 Toulouse cedex 9, France

²Laboratoire de Spectroscopie Atomique, Moléculaire et Applications (LSAMA), Faculté des Sciences de Tunis, Université de Tunis el Manar, 1060 Tunis, Tunisia

Abstract A method based upon the weighted total cross section (WTCS) theory is proposed to calculate the photo-ionisation cross sections and the radiative recombination rate coefficients between the fundamental level of CO and the main electronic states of its corresponding ion. Total photo-ionisation cross sections and radiative recombination rate coefficients are determined from the calculation of elementary vibrational photo-ionisation cross sections. Transitions between CO⁺(X, A and B) and CO(X) are considered. Total photo-ionisation cross sections and recombination coefficients are computed in the temperature interval 500-15000 K.

Keywords: CO, photo-ionisation cross sections, radiative recombination rate coefficients

PACS: 52.20.-j, 82.33.Xj

DOI: 10.1088/1009-0630/16/11/04

(Some figures may appear in colour only in the online journal)

1 Introduction

Carbon-oxygen containing plasmas are involved in many electric arc processes or applications. One can mention for example: **a.** low voltage circuit breakers with mixtures of air and organic vapours (C_wH_xO_yN_z) due to thermoplastic wall erosion [1–3], **b.** high-voltage breaking devices with Air-CO₂-C_xF_y mixtures as an alternative to SF₆ [4], **c.** biomass treatment for syngas [5], CO₂-N₂-Ar mixtures for the study of planetary atmosphere re-entry [6–10], and **d.** Metal Inert Gas (MIG)-Metal Active Gas (MAG) welding arcs with Ar-CO₂ mixtures [11].

These processes have been widely studied theoretically, mainly through the implementation of Magneto-Hydro-Dynamic (MHD) Models (Ref. [12] and references therein) with the hypothesis of local thermodynamic equilibrium (LTE). On the other hand, we know that the LTE assumption is no longer acceptable in some locations inside the plasma where deviations from thermal, chemical or radiative equilibrium may exist: close to the electrodes and the walls and in the surrounding areas of the arc where turbulence phenomena and the pumping of external gas have a significant effect. Moreover, LTE is not always valid during arc extinction and inside the plasma column for low-power arcs. For a theoretical study of this kind of plasma for which departures from equilibrium may exist, multi-temperature MHD models are developed. Several articles are available in the literature concerning

2T MHD models such as Bernardi et al. [13], El Morsli and Proulx [14], Tanaka [15] and Al Mamun et al. [16] concerning respectively argon, air, Ar-N₂ and Ar-CO₂-H₂ radio-frequency inductively coupled plasma (ICP) torches, Ghorui et al. [17] for the study of the gas flow inside the nozzle of a metal cutting device, Belhaouari et al. [18] associated to SF₆ high voltage circuit breakers and Trelles et al. [19] for the study of a direct current (DC) plasma torch in argon. The development of this kind of model is based upon multi-temperature thermodynamic properties and transport coefficients databases. It is thus indispensable to calculate these properties and the first step, impossible to circumvent, is the calculation of the plasma composition. Moreover, the only accurate way to obtain the plasma composition, with the existence of departures from thermal, chemical or radiative equilibrium, is to adopt a collisional-radiative (CR) model [20]. These models are based on chemical species conservation equations established from direct and reverse chemical reactions occurring in the plasma. As a consequence, it is necessary to have a complete set of cross sections or reaction rate coefficients to develop appropriate CR models. Rate coefficients are often found from a literature survey but some of them, particularly concerning excited electronic levels of molecular species, are unavailable and have to be determined theoretically. This work is connected with this problem as it concerns the calculation of photo-ionisation cross sections and radiative recombination rate coefficients for the CO molecule (and

its corresponding ion) which is a dominant diatomic species for C-O containing plasmas.

It is essential to take account of radiative mechanisms in CR models (mainly spontaneous emission and radiative recombination). Indeed, these processes make it possible to highlight the possible presence of departures from radiative equilibrium. In previous works performed in our laboratory for nitrogen [21], oxygen [22] and air [20,23,24], it has been established that some atomic or molecular electronic states are under populated due to radiation losses (in these previous studies, radiative recombination rate coefficients for N₂, O₂ and NO molecules were calculated, as in the present work, in the frame of the Weighted Total Cross Section (WTCS) theory [25]). Thus, it is indispensable to include radiative processes in the kinetic scheme of CR models in order to obtain reliable results. On the other hand, there also exist CR models devoted to the study of planetary entry plasmas [10] for earth (air) and mars (CO₂-N₂-Ar) atmospheres for which radiative recombination of molecular electronic states is not taken into account. Rate coefficients calculated in the present work for CO molecules could be used to improve these CR models.

Concerning radiative recombination rate coefficients, we did not find any articles for CO⁺. On the other hand, theoretical [26,27] or experimental [28–30] photo-ionisation cross sections have been already published for CO. Moreover, reference should be made to the review by Gallagher et al [31]. However, this kind of cross section cannot be used to calculate accurate radiative recombination rate coefficients for molecular electronic levels in the case of thermal or quasi-thermal plasmas. Indeed, these previous experimental or theoretical cross sections were obtained from (or considering) photon collisions on a cold gas. As a consequence, the target molecule was in its fundamental state (electronic ground level X and vibrational quantum number $v = 0$), whereas the population of electronic and vibrational levels follows a Boltzmann distribution in thermal plasmas. Thus, it is crucial to determine photo-ionisation cross sections as a function of vibrational quantum numbers and temperature to undertake accurate computations of radiative recombination rate coefficients for CO⁺ electronic levels.

In the present work, photo-ionisation cross sections are determined according to the Weighted Total Cross Section (WTCS) theory [25]. Radiative recombination rate coefficients for the electronic levels of CO⁺ (X, A and B) are then calculated from photo-ionisation cross sections with the assumption of a Maxwell-Boltzmann velocity distribution function for electron and heavy particles.

2 Theory and methods

From the works of Marr [32] and Bates [33], with the assumption of a Maxwell-Boltzmann velocity distribution function for electrons and heavy particles, the ra-

diative recombination rate coefficient $\beta(\text{m}^3 \cdot \text{s}^{-1})$ is obtained as a function of temperature θ from the total photo-ionisation cross section $\sigma_{T_1}^{T_2}(\varepsilon, \theta)$ (where T_1 is the electronic state of the neutral molecule CO and T_2 the electronic level of the molecular ion CO⁺):

$$\begin{aligned} \beta_{T_1}^{T_2}(\theta) &= \frac{D_{T_1}(\theta)}{D_{T_2}(\theta)} \sqrt{\frac{2}{\pi}} \frac{1}{c^2 (m_e k)^{3/2}} \times \theta^{-3/2} \\ &\times \exp\left(\frac{E_{T_2}(\theta) - E_{T_1}(\theta)}{k\theta}\right) \\ &\times \int_{\varepsilon_{\text{threshold}}}^{\infty} \varepsilon^2 \sigma_{T_1}^{T_2}(\varepsilon, \theta) \exp\left(-\frac{\varepsilon}{k\theta}\right) d\varepsilon, \quad (1) \end{aligned}$$

where c is the speed of light, m_e is the electron mass and k is Boltzmann's constant. ε is the energy of the photon and $\varepsilon_{\text{threshold}}$ is the energy threshold of the transition ($T_1 \rightarrow T_2$). $E_{T_i}(\theta)$ and $D_{T_i}(\theta)$ are respectively the energy and the degeneracy of the coalesced molecular electronic level T_i . Their calculation is achieved according to Refs. [21,34]. The energy for a coalesced electronic level T_i is given by:

$$E_{T_i}(\theta) = T_{e_i} + \langle G(v_i) + F_{v_i}(J_i) \rangle_{\theta}, \quad (2)$$

with:

$$\begin{aligned} &\langle G(v_i) + F_{v_i}(J_i) \rangle_{\theta} \\ &= \frac{1}{q(T_i, \theta)} \times \sum_{v_i=0}^{v_L(T_i)} \sum_{J_i=0}^{J_L(v_i)} (2J_i + 1) (G(v_i) \\ &+ F_{v_i}(J_i)) \exp\left(-\frac{G(v_i) + F_{v_i}(J_i)}{k\theta}\right). \quad (3) \end{aligned}$$

And the degeneracy of a coalesced level is written as:

$$\begin{aligned} D_{T_i}(\theta) &= (2 - \delta_{0,\Lambda})(2S + 1)q(T_i, \theta) \\ &\times \exp\left(\frac{\langle G(v_i) + F_{v_i}(J_i) \rangle_{\theta}}{k\theta}\right). \quad (4) \end{aligned}$$

S is the electron spin quantum number and Λ is the quantum number associated to the angular orbital moment. $F_{v_i}(J_i)$ and $G(v_i)$ are respectively the energy of the rotational level J_i and of the vibrational level v_i . They are given by [35,36]:

$$G(v) = (v + \frac{1}{2}) \omega_e - (v + \frac{1}{2})^2 \omega_e x_e + (v + \frac{1}{2})^3 \omega_e y_e + \dots \quad (5)$$

$$F_v(J) = B_v J(J + 1) - D_v J^2 (J + 1)^2, \quad (6)$$

with $B_v = B_e - \alpha_e (v + \frac{1}{2})$ and $D_v = D_e + \beta_e (v + \frac{1}{2})$. T_e , B_e , α_e , D_e , β_e , ω_e , $\omega_e x_e$ and $\omega_e y_e$ are spectroscopic constants taken from Refs. [37, 38] and summarized in Table 1 for CO and CO⁺. In relations (3) and (4), $q(T_i, \theta)$ is the internal partition function of the particular electronic state T_i . It is written as [36]:

$$q(T_i, \theta) = \sum_{v_i=0}^{v_L(T_i)} \sum_{J_i=0}^{J_L(v_i)} (2J_i + 1) \exp\left(-\frac{G(v_i) + F_{v_i}(J_i)}{k\theta}\right). \quad (7)$$

Table 1. Spectroscopic data of CO and CO⁺ electronic levels

State	T_e	ω_e	$\omega_e x_e$	$\omega_e y_e$	r_e	D_0	B_e	α_e	D_e	β_e
	(cm ⁻¹)	(cm ⁻¹)	(cm ⁻¹)	(cm ⁻¹)	(10 ⁻⁸ cm)	(cm ⁻¹)	(cm ⁻¹)	(cm ⁻¹)	(cm ⁻¹)	(cm ⁻¹)
CO ⁺ B ² Σ ⁺	158907.2	1734.18	27.927	0.3283	1.16877	37241.0	1.79992	0.03025	7.76×10 ⁻⁶	2.60×10 ⁻⁷
CO ⁺ A ² Π _i	133763.8	1562.06	13.532	0.0131	1.24377	46516.7	1.58940	0.01942	6.58×10 ⁻⁶	1.38×10 ⁻⁸
CO ⁺ X ² Σ ⁺	113030.5	2214.24	15.164	-0.0007	1.11514	67250.0	1.97720	0.01896	6.31×10 ⁻⁶	1.61×10 ⁻⁸
COX ¹ Σ ⁺	0.0	2169.81	13.238	0.0105	1.12832	89460.0	1.93128	0.0175	6.12×10 ⁻⁶	-1.04×10 ⁻⁹

The global photo-ionisation cross section involved in Eq. (1) for the transition between two electronic states $T_1 \rightarrow T_2$ is calculated in the frame of the WTCS theory [25] such as:

$$\sigma_{T_1}^{T_2}(\varepsilon, \theta) = \frac{\sum_{v_1=0}^{v_L(T_1)} n(T_1, v_1, \theta) \times \sum_{v_2=0}^{v_L(T_2)} \sigma_{T_1, v_1}^{T_2, v_2}(\varepsilon)}{n(T_1, \theta)}, \quad (8)$$

where $n(T_1, v_1, \theta)$ and $n(T_1, \theta)$ are respectively the population number density of the vibrational and electronic levels. With the assumption that electronic, vibrational and rotational levels follow a Boltzmann distribution, $n(T_1, v_1, \theta)$ and $n(T_1, \theta)$ can be expressed in the thermal equilibrium case as a function of partition functions, and vibrational and rotational energies (cf. references [36,39] for detailed expressions of $n(T_1, v_1, \theta)$ and $n(T_1, \theta)$). With this additional hypothesis, the weighted total photo-ionisation cross section is finally written as [39]:

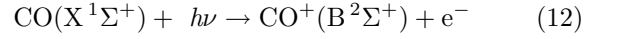
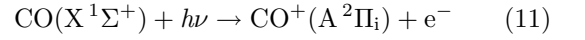
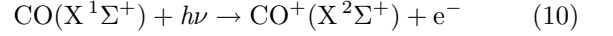
$$\sigma_{T_1}^{T_2}(\varepsilon, \theta) = \sum_{v_1=0}^{v_L(T_1)} \frac{1}{B_{v_1}} \exp\left(-\frac{G(v_1)}{k\theta}\right) \times \sum_{v_2=0}^{v_L(T_2)} \sigma_{T_1, v_1}^{T_2, v_2}(\varepsilon) \bigg/ \sum_{v_1=0}^{v_L(T_1)} \frac{1}{B_{v_1}} \exp\left(-\frac{G(v_1)}{k\theta}\right), \quad (9)$$

where $\sigma_{T_1, v_1}^{T_2, v_2}(\varepsilon)$ is the elementary vibrational photo-ionisation cross section. It is determined according to Sarrette et al. [40] and Skubenich et al [41]. All the details concerning the method of calculation of $\sigma_{T_1, v_1}^{T_2, v_2}(\varepsilon)$ are available in Ref. [39]. In order to achieve the computation of the elementary vibrational photo-ionisation cross section $\sigma_{T_1, v_1}^{T_2, v_2}(\varepsilon)$, the Franck-Condon factors $q_{v_1 v_2}$ are indispensable. In this study, Franck-Condon factors are taken from Ref. [42]. These authors give Franck-Condon factors for the following vibrational transitions: CO(X, $v_1=0-24$) \rightarrow CO⁺(X, $v_2=0-13$), CO(X, $v_1=0-24$) \rightarrow CO⁺(A, $v_2=0-10$) and CO(X, $v_1=0-24$) \rightarrow CO⁺(B, $v_2=0-10$).

3 Results and discussion

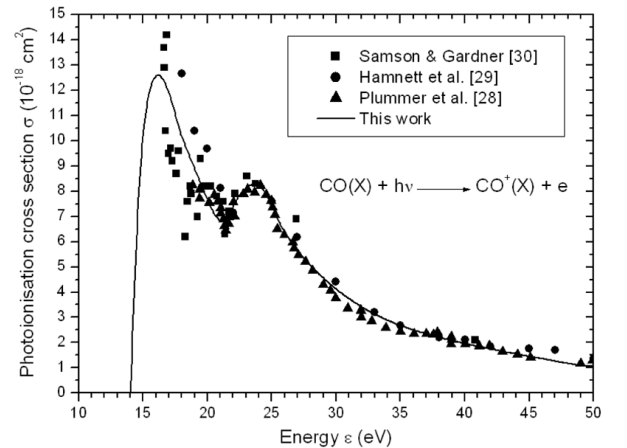
In order to validate our computations, we have confronted our weighted total photo-ionisation cross sections $\sigma_{T_1}^{T_2}(\varepsilon, \theta)$ (obtained for $\theta = 300$ K) with available

measurements [28–30] in Figs. 1, 2 and 3, respectively for the ensuing reactions:



As stated previously, the aim of the present work is to determine the radiative recombination rate coefficients which are strongly correlated with the energy threshold and with the low-energy cross section shape. From Figs. 1-3, one can notice that our results and previous measurements exhibit an acceptable agreement, in particular for the position and the value of the maximum of the cross section, and for the energy threshold.

In Figs. 1-3, we can observe that the cross sections do not exhibit one unique maximum but rather two peaks. The appearance of this second maximum is due to a phenomenon called shape resonance [43]. These shape resonances for CO molecules are clearly identified in the photo-ionisation spectra of states X [44,45], A [44] and B [45–47]. The peaks associated with shape resonances are located near 23.5 eV, 22 eV and 32 eV for states X, A and B, respectively, and they are well reproduced in our calculations.


Fig.1 300 K photo-ionisation WTCS for CO(X¹Σ⁺) \rightarrow CO⁺(X²Σ⁺)

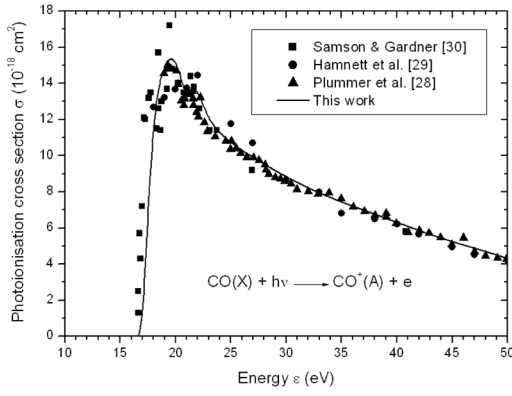


Fig.2 300 K photo-ionisation WTCS for $\text{CO}(X^1\Sigma^+) \rightarrow \text{CO}^+(A^2\Pi_i)$

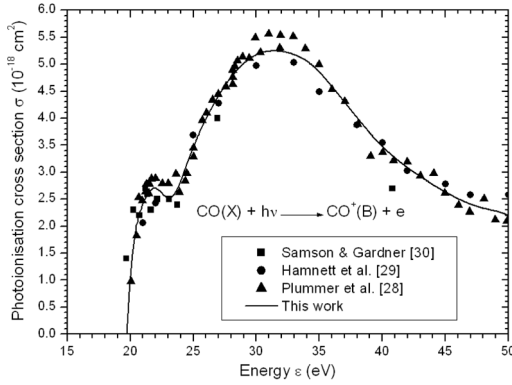


Fig.3 300 K photo-ionisation WTCS for $\text{CO}(X^1\Sigma^+) \rightarrow \text{CO}^+(B^2\Sigma^+)$

In order to obtain radiative recombination rate coefficients, it is necessary to calculate total photo-ionisation cross sections as a function of temperature. For all the processes studied, the same variation of the photo-ionisation cross section was observed with temperature: a decrease of the maximum value and a threshold shift towards low energies, as shown in Figs. 4 to 6 respectively for the 3 mechanisms considered in this work, i.e. reactions (10) to (12).

However, the effect of temperature upon the total cross section is more or less significant, depending on the process considered. Indeed, for the transition $\text{CO}(X^1\Sigma^+) \rightarrow \text{CO}^+(X^2\Sigma^+)$ (see Fig. 4), the variation of the cross section maximum value is only about 12% (for temperatures varying between 500 K and 15000 K), whereas it is close to a factor of 1.6 for $\text{CO}(X^1\Sigma^+) \rightarrow \text{CO}^+(A^2\Pi_i)$ (see Fig. 5).

The threshold shift toward low energy (for increasing temperature) of the total photo-ionisation cross section $\sigma_{T_1}^{T_2}(\epsilon, \theta)$ is associated to the population number densities of high vibrational levels. Indeed, when the temperature increases, according to Boltzmann's law, the population of high vibrational levels v_1 and v_2 becomes non-negligible, leading to a lowering of the energy threshold of the process.

In addition, the modification with temperature of the maximum value of the total photo-ionisation cross section arises from the elementary vibrational photo-

ionisation cross sections $\sigma_{T_1, v_1}^{T_2, v_2}(\epsilon)$ and from the Franck-Condon factors whose values can vary significantly (several orders of magnitude) with regards to the electronic transition and to the couple of vibrational quantum numbers v_1 and v_2 (in particular, for increasing temperatures i.e. for high values of v_1 and v_2).

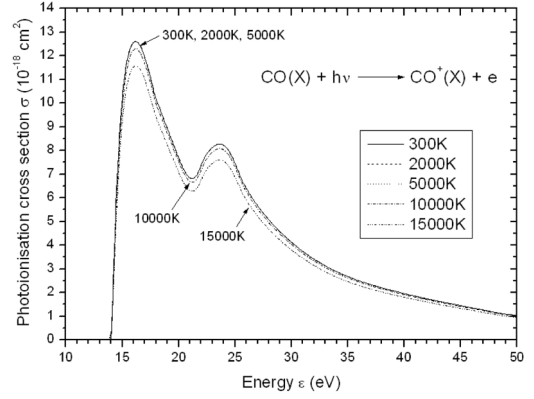


Fig.4 WTCS for $\text{CO}(X^1\Sigma^+) \rightarrow \text{CO}^+(X^2\Sigma^+)$ as a function of temperature

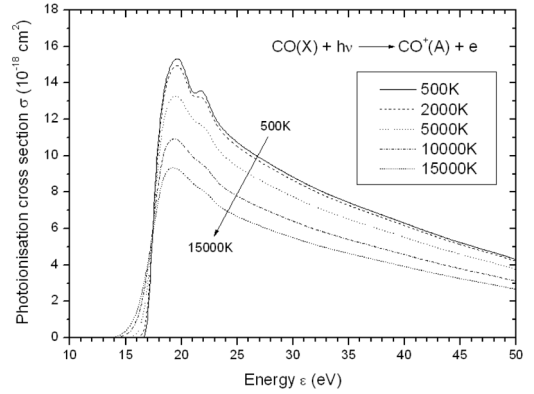


Fig.5 WTCS for $\text{CO}(X^1\Sigma^+) \rightarrow \text{CO}^+(A^2\Pi_i)$ as a function of temperature

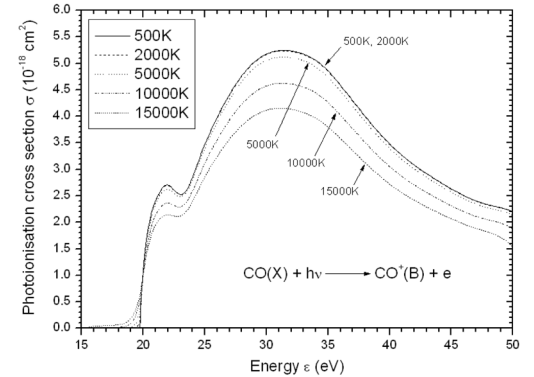


Fig.6 WTCS for $\text{CO}(X^1\Sigma^+) \rightarrow \text{CO}^+(B^2\Sigma^+)$ as a function of temperature

Radiative recombination rate coefficients $\beta_{T_1}^{T_2}(\theta)$ obtained in this study are presented in Fig. 7 as a function of temperature for the reactions (10), (11) and (12). These rate coefficients are typically in the range of 10^{-13} - 10^{-14} cm^3/s , and they are slowly varying with temperature. This last result is not surprising since radiative recombination is an exothermic process.

Table 2. Fitting parameters (6th degree polynomial) of CO⁺ radiative recombination rate coefficients: $\beta_{T_1}^{T_2}$ (cm³ · s⁻¹) = $a_0 + a_1 \times \theta + a_2 \times \theta^2 + \dots + a_6 \times \theta^6$ with θ in Kelvin

Recombination process	Fitting parameters
CO ⁺ (X ² Σ ⁺) + e ⁻ → CO(X ¹ Σ ⁺) + hν	$a_0 = 1.0908 \times 10^{-14}$, $a_1 = 2.1044 \times 10^{-17}$ $a_2 = -4.6750 \times 10^{-21}$, $a_3 = 6.4780 \times 10^{-25}$ $a_4 = -5.3648 \times 10^{-29}$, $a_5 = 2.3419 \times 10^{-33}$ $a_6 = -4.1118 \times 10^{-38}$
CO ⁺ (A ² Π _i) + e ⁻ → CO(X ¹ Σ ⁺) + hν	$a_0 = 5.6988 \times 10^{-15}$, $a_1 = 1.1574 \times 10^{-17}$ $a_2 = -1.8661 \times 10^{-21}$, $a_3 = 1.1234 \times 10^{-25}$ $a_4 = -7.9925 \times 10^{-31}$, $a_5 = -1.8235 \times 10^{-34}$ $a_6 = 5.4547 \times 10^{-39}$
CO ⁺ (B ² Σ ⁺) + e ⁻ → CO(X ¹ Σ ⁺) + hν	$a_0 = 1.2032 \times 10^{-15}$, $a_1 = 1.5090 \times 10^{-17}$ $a_2 = -3.6145 \times 10^{-21}$, $a_3 = 4.8036 \times 10^{-25}$ $a_4 = -3.8353 \times 10^{-29}$, $a_5 = 1.6725 \times 10^{-33}$ $a_6 = -2.9986 \times 10^{-38}$

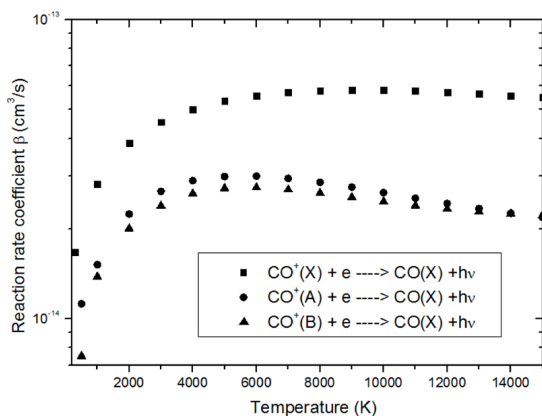


Fig. 7 Radiative recombination rate coefficients $\beta_{T_1}^{T_2}(\theta)$ of the electronic levels of CO⁺

Unfortunately, we did not find any theoretical or experimental published value of radiative recombination rate coefficients for CO⁺ ions to confront and validate our own calculation.

The rate coefficients obtained in this study were also fitted in a polynomial form (valid in the temperature interval 500-15000 K): $\beta_{T_1}^{T_2}$ (cm³ · s⁻¹) = $a_0 + a_1 \times \theta + a_2 \times \theta^2 + \dots + a_6 \times \theta^6$. The fitting parameters (a_i) are given in Table 2.

4 Conclusions

A theoretical approach allowing the computation of photo-ionisation cross sections and radiative recombination rate coefficients for electronic states of diatomic molecules is presented. This method is applied in the present work to the transitions CO⁺(X, A and B) → CO(X). Total photo-ionisation cross sections are calculated in the frame of the weighted total cross section theory [25]. They are obtained from elementary vibrational photo-ionisation cross sections and Franck-Condon factors. Radiative recombination rate coeffi-

cients are then determined from photo-ionisation cross sections with the assumption of Maxwell-Boltzmann velocity distribution functions for electrons and heavy particles. Calculations are realized in the temperature interval 500-15000 K and fitting parameters are given for the rate coefficients in a polynomial form: β (cm³ · s⁻¹) = $a_0 + a_1 \times \theta + a_2 \times \theta^2 + \dots + a_6 \times \theta^6$. The room-temperature photo-ionisation cross sections computed in this work were also confronted with experimental published values in order to validate our own calculations.

The database of photo-ionisation cross sections obtained in this study can be used for any kind of plasma, whereas reaction rate coefficients are only usable in the case of thermal or quasi thermal plasmas for which the assumption of Maxwell-Boltzmann velocity distribution functions is effective.

These data can also be used to develop a collisional-radiative model for C-O containing plasmas in order to obtain the plasma composition, taking into account the existence of departures from thermal and chemical equilibrium. The composition will then be used to obtain multi-temperature thermodynamic properties and transport coefficients.

The set of photo-ionisation cross sections calculated in this study can also be used to improve the photo-absorption cross section database necessary for the calculation of the molecular continuum contribution to radiative properties of thermal plasmas such as the net emission coefficient [48] or mean absorption coefficients [49].

Acknowledgments

The authors acknowledge the “Comité Mixte Franco-Tunisien pour la Coopération Universitaire (Partenariat Hubert Curien, Utique, Tunisie)” for its financial support in the achievement of this work.

List of symbols

Symble	Unit	Description
c	$(\text{m}\cdot\text{s}^{-1})$	Speed of light
$D_{T_i}(\theta)$		Degeneracy of the coalesced molecular electronic state T_i
$E_{T_i}(\theta)$	(J)	Energy of the coalesced molecular electronic state T_i
$F_v(J)$	(J)	Energy of rotational level J
$G(v)$	(J)	Energy of vibrational level v
J_i		Rotational quantum number of state (T_i, v_i)
k	(J/K)	Boltzmann's constant
m_e	(kg)	Electron mass
$n(T_i, \theta)$	(m^{-3})	Population number density of electronic state T_i
$n(T_i, v_i, \theta)$	(m^{-3})	Population number density of vibrational state v_i
$q(T_i, \theta)$		Internal partition functions of electronic state T_i
$q_{v_1 v_2}$		Franck-Condon factor for transition $v_1 \rightarrow v_2$
S		Electron spin quantum number
T_i	(J)	Electronic term of electronic level i
v_1		Vibrational quantum number of state T_1
v_2		Vibrational quantum number of state T_2
$\beta_{T_1}^{T_2}(\theta)$	$(\text{m}^3\cdot\text{s}^{-1})$	Radiative recombination rate coefficient for transition $T_1 \rightarrow T_2$
δ		Kronecker's symbol
ε	(J)	Energy of the incoming photon
Λ		Quantum number associated to the angular orbital moment
$\sigma_{T_1, v_1}^{T_2, v_2}$	(m^2)	Vibrational photo-ionisation cross section for transition $(T_1, v_1) \rightarrow (T_2, v_2)$
$\sigma_{T_1}^{T_2}(\varepsilon, \theta)$	(m^2)	Weighted total photo-ionisation cross section for transition $T_1 \rightarrow T_2$
θ	(K)	Temperature

References

- Teulet Ph, Gonzalez J J, Mercado-Cabrera A, et al. 2009, J. Phys. D: Appl. Phys., 42: 175201
- Teulet Ph, Gonzalez J J, Mercado-Cabrera A, et al. 2009, J. Phys. D: Appl. Phys., 42: 185207
- André P, Brunet L, Bussiére W, et al. 2004, Eur. Phys. J. Appl. Phys., 25: 169
- Cressault Y, Connord V, Hingana H, et al. 2011, J. Phys. D: Appl. Phys., 44: 495202
- Aubretton J, Elchinger M F, Hacala A, et al. 2009, J. Phys. D: Appl. Phys., 42: 095206
- Drake D J, Popovic S, Vuskovic L, et al. 2009, IEEE Trans. Plasma Sci., 37: 1646
- Bultel A, Chéron B G, Bourdon A, et al. 2006, Physics of Plasmas, 13: 043502
- Colonna G, D'Angola A, Laricchiuta A, et al. 2013, Plasma Chem. Plasma Process., 33: 401
- Colonna G, D'Angola and Capitelli M. 2012, Physics of Plasmas, 19: 072115
- Bultel A and Annaloro J. 2013, Plasma Sources Sci. Technol., 22: 025008
- Zielinska S, Pellerin S, Valensi F, et al. 2008, Eur. Phys. J. Appl. Phys., 43: 111
- Gleizes A, Gonzalez J J and Freton P. 2005, J. Phys D: Appl. Phys., 38: R153
- Bernardi D, Colombo V, Coppa G G M, et al. 2001, Eur. Phys. J. D, 14: 337
- El Morsli M and Proulx P. 2007, J. Phys. D: Appl. Phys., 40: 4810
- Tanaka Y. 2004, J. Phys. D: Appl. Phys., 37: 1190
- Al-Mamun S A, Tanaka Y and Uesugi Y. 2010, Plasma Chem. Plasma Process., 30: 141
- Ghorui S, Heberlein J V R and Pfender E. 2007, J. Phys. D: Appl. Phys., 40: 1966
- Belhaouari J B, Gonzalez J J and Gleizes A. 1998, J. Phys. D: Appl. Phys., 31: 1219
- Trelles J P, Heberlein J V R and Pfender E. 2007, J. Phys. D: Appl. Phys., 40: 5937
- Teulet Ph, Sarrette J P and Gomes A M. 2001, J. Quant. Spectrosc. Radiat. Transfer, 70: 159
- Bacri J, Lagreca M and Medani A. 1982, Physica C, 113: 403
- Gomes A M, Essoltani A and Bacri J. 1990, J. Quant. Spectrosc. Radiat. Transfer, 43: 471
- Sarrette J P, Gomes A M and Bacri J. 1995, J. Quant. Spectrosc. Radiat. Transfer, 53: 125
- Sarrette J P, Gomes A M and Bacri J. 1995, J. Quant. Spectrosc. Radiat. Transfer, 53: 143
- Bacri J and Médani A. 1980, Physica C, 101: 399
- Rescigno T N, Lengsfield B H and Orel A E. 1993, J. Chem. Phys., 99: 5097

- 27 Kilcoyne D A L, Nordholm S and Hush N S. 1986, Chem. Phys., 107: 225
- 28 Plummer E W, Gustafsson T, Gudat W, et al. 1997, Phys. Rev. A, 15: 2339
- 29 Hamnett A, Stoll W and Brion C E. 1976, J. Electron Spectrosc. Relat. Phenomena, 8: 367
- 30 Samson J A and Gardner J L. 1976, J. Electron Spectrosc. Relat. Phenomena, 8: 35
- 31 Gallagher J W, Brion C E, Samson J A R, et al. 1988, J. Phys. Chem. Ref. Data, 17: 9
- 32 Marr G V. 1967, Photoionization processes in gases; Pure and Applied Physics. Academic Press, New-York, London
- 33 Bates D R. 1962, Atomic and molecular processes. Academic Press, New-York, London
- 34 Teulet Ph. 1998, Etude des écarts à l'équilibre radiatif et thermique dans les plasmas air et air – sodium. Application au diagnostic spectroscopique. Ph. D. Thesis n°3298, Université Paul Sabatier Toulouse 3 (France) (in French)
- 35 Drellishak K S, Aeschliman D P and Cambel A Bulent, 1965, Phys. Fluids, 8: 1590
- 36 Capitelli M, Colonna G and D'Angola A. 2011, Fundamental Aspects of Plasma Chemical Physics, Thermodynamics, Springer Series in Atomic, Optical, and Plasma Physics, Springer, New York, ISBN 978-1-4419-8181-3
- 37 Babou Y, Rivière Ph, Perrin M Y, et al. 2009, J. Quant. Spectrosc. Radiat. Transfer, 110: 89
- 38 Huber K P and Herzberg G. 1978, Molecular Spectra and Molecular structure. IV Constants of Diatomic Molecules. Van Nostrand Reinhold, New York
- 39 Riahi R, Teulet Ph, Cressault Y, et al. 2008, Eur. Phys. J. D, 49: 185
- 40 Sarrette J P, Gomes A M and Bacri J. 1992, Journal of High Temperature Chemical Processes, Colloque, supplément au n°3, 1: 403 (in French)
- 41 Skubenich V V, Povch M M and Zapesochnyi I P. 1977, High Energy Chemistry, 11: 92
- 42 Nicholls R W. 1968, J. Phys. B: At. Mol. Opt. Phys., 1: 1192
- 43 Piancastelli N M. 1999, J. Electron Spec. Relat. Phenom., 100: 167
- 44 Zhong Z P and Li J M. 2004, J. Phys. B: At. Mol. Opt. Phys., 37: 735
- 45 Lopez-Dominguez J A, Hardy D, Das R, et al. 2012, J. Electron Spec. Relat. Phenom., 185: 211
- 46 Farquar G R, Miller J S, Poliakov E D, et al. 2001, J. Chem. Phys., 115: 9764
- 47 Das R, Wu C, Mihill A G, et al. 1995, J. Phys. Chem., 99: 1741
- 48 Naghizadeh-Kashani Y, Cressault Y and Gleizes A. 2002, J. Phys. D: Appl. Phys., 35: 2925
- 49 Cressault Y and Gleizes A. 2006, High Temp. Mat. Proc., 10: 47

(Manuscript received 22 July 2013)

(Manuscript accepted 5 November 2013)

E-mail address of corresponding author

Philippe TEULET: philippe.teulet@laplace.univ-tlse.fr